Journal of Sound and Vibration 329 (2010) 4354–4366

Contents lists available at ScienceDirect

Journal of Sound and Vibration

journal homepage: www.elsevier.com/locate/jsvi

Modelling and design of a novel air-spring for a suspension seat

Marco W. Holtz, Johannes L. van Niekerk *

Sound & Vibration Research Group, Department of Mechanical and Mechatronic Engineering, Stellenbosch University, South Africa

ARTICLE INFO

Article history:
Received 15 December 2008
Received in revised form
15 April 2010
Accepted 16 April 2010
Handling Editor: M.P. Cartmell
Available online 8 June 2010

ABSTRACT

Air-springs used in conjunction with auxiliary volumes provide both spring stiffness and damping. The damping is introduced through the flow restriction connecting the two air volumes. This article presents a simplified model of an air-spring with an auxiliary volume derived from first principles for simulation and design of an air-spring coupled to an auxiliary volume for a suspension seat. Tests were performed on an experimental apparatus to validate the model. The simulation model of the air-spring and auxiliary volume followed the trend predicted by the literature but showed approximately 27% lower transmissibility amplitude and 21% lower system natural frequency than that obtained by tests when using large diameter flow restrictions. This inaccuracy is assumed to be introduced by the simplified mass transfer equations defining the flow restriction between air-spring and auxiliary volume. The model showed closer correlation to the experimental results when the auxiliary volume size was decreased by two-thirds of the volume actually used for the experiment. A procedure, using the developed simulation model, for the design of a prototype air-spring and auxiliary volume, is presented for application in a typical articulated or rigid frame dump truck. The goal of the study was to design a suspension seat for this application and to obtain a SEAT value below 1.1. The design was optimised by varying auxiliary volume size and flow restriction diameters for different loads. A SEAT value of less than 0.9 was achieved, clearly indicating the effectiveness of using an auxiliary volume with an air-spring as seat suspension.

1. Introduction

Vibrations are encountered by any vehicle as it is driven over irregular road surfaces. As the loading capacities of earth-moving equipment increase, as well as the speed at which these vehicles travel, stiffer suspensions are required, resulting in larger vibration inputs to the structure of the vehicle, and especially the driver, who spends long hours in the vehicle. These design measures to improve productivity have resulted in both the vehicle body and the human occupants being subjected to higher levels of vibration, and ensuing discomfort and fatigue.

Until recently no legislation governing whole body vibration exposure existed, and suspension systems were designed to what was considered to be ''reasonable'' vibration exposure levels. Studies have shown that in certain cases suspension systems amplified the vibrations between 0 and 20 Hz by as much as four times and as many as 45% of seats used in industry increase, rather than decrease, the accelerations, mainly due to end-stop impacts [1]. Research on the health risks of vibration exposure has led to a revision of legislation and the development of the Physical Agents (Vibration) Directive by the European Union [2]. Included in this directive is an exposure action value (EAV) of 0.5 m/s^2 rms (or 9.1 $m/s^{1.75}$ VDV),

* Corresponding author. Tel.: +27 21 808 4251.
E-mail address: wikus@sun.ac.za (J.L. van Niekerk).

0022-460X/$ - see front matter © 2010 Elsevier Ltd. All rights reserved.
doi:10.1016/j.jsv.2010.04.017

Nomenclature

A	area
A_s	heat transfer area
C_v	specific heat for constant volume process
c	damping constant
d	flow restriction diameter
e	wall roughness
f	applied force(s) in equation of motion
f_{loss}	friction factor
g	gravitational acceleration
Q	heat transfer coefficient
P_{loss}	pressure loss
x	height of spring
h_{enth}	enthalpy
$\dot{x}$	rate of change of spring deflection
K_E	expansion loss coefficient
K_C	contraction loss coefficient
l	flow restriction length
m_l	suspended mass
m	air mass
$\dot{m}$	air mass flow rate
n	ratio of specific heats/constant for polytrophic process
P_a	atmospheric pressure
P	internal pressure
R	gas constant
T_s	temperature of heat transfer surface
T	temperature
$\dot{T}$	rate of temperature change
V	volume
y	total/absolute piston displacement
$\dot{y}$	total piston velocity
$\ddot{y}$	total piston acceleration
z	total/absolute base displacement
$\dot{z}$	total base velocity

Abbreviations

EAV	exposure action value
ELV	exposure limit value
ISO	International Standards Organisation
rms	root mean square
SEAT	seat effective amplitude transmissibility
VDV	vibration dose value
WBV	whole body vibration

The subscripts '1' and '2' used in the text and equations refer to the air-spring and auxiliary volume, respectively. The subscript '0' refers to reference or equilibrium conditions and '*r*' is used to identify relative temperature or pressure. No numerical subscript indicates a constant value.

which determines what a "reasonable" level of exposure is over 8-hour workday and an exposure limit value (ELV) of 1.15 m/s^2 rms (or 21 m/s$^{1.75}$ VDV), which may not be exceeded over an 8-hour working day [2].

Typical vibrations experienced by occupants in off-road vehicles are at low frequencies between 1 and 10 Hz and high amplitudes of about 1.5 m/s^2. It is well known that these vibrations can cause or aggravate physical symptoms that impair driver health in predominantly two major areas: gastric complaints and spinal disorders [3–5].

In attempting to reduce these problems, particular attention has been focused on reducing vibrations transmitted to the operator by isolating the vehicle operator from vibration and large amplitude shock excitations transmitted by the vehicle. This was accomplished by adding seat and cab suspensions to vehicles. As seats are the final mechanisms where the operator can be isolated from the vehicle vibration, this article deals with the design of a novel air-spring for a seat suspension.

To attenuate vibrations transmitted to the occupant, suspension seats have generally been used in the conventional coil spring and hydraulic damper combination. To further improve on these suspensions, air-spring technology, initially used in vehicle suspensions, was introduced. The reasons for the increased popularity of air-springs compared to the conventional coil spring and damper suspensions as presented in Quaglia and Sorli [6] are their

- adjustable carrying capacity;
- reduced weight;
- variable spring rate with constant 'tuned' frequency;
- reduced structurally transmitted noise; and
- variable ride height.

When using air-springs in suspension systems, they predominantly exhibit stiffness and, as with conventional coil springs, require additional damping. However, to eliminate the need for an additional hydraulic damper, the use of air-springs in conjunction with auxiliary volumes has been proposed [1,6]. In most instances, these systems are made up of the bellows or diaphragm air-spring connected to an auxiliary reservoir by a thin tube offering resistance to the flow of air. The interaction between these two air volumes and the resistance between them determines the frequency response of the system, particularly a shift in resonant frequency and change of magnitude in the transmitted vibration [6]. The aim is thus to find the correct resistance value for the specific air-spring/auxiliary volume ratio to place the transmissibility peak at the lowest amplitude, and thereby the resistance introduces sufficient damping into the system to eliminate the need for additional hydraulic dampers.

In order to design prototype air-spring suspension systems, accurate models need to be developed. Air-springs and auxiliary volumes however are difficult to model in comparison to the traditional coil springs due to the various non-linear characteristics they exhibit. This can be attributed to the fact that a gas is used as the component providing the stiffness, thereby introducing thermodynamic, heat transfer and fluid mechanic effects into the model. Improvements have been made in the accuracy of the spring models by incorporating these effects [7].

Various methods incorporating the above mentioned effects have been devised to generate models that will accurately determine the response of springs to different input excitation frequencies and magnitudes. Qauglia and Sorli [8] derived the stiffness of their air-spring model based on the basic force–distance relationship. Considering that the force can be attributed to the air pressure inside the spring and the area this pressure acts on, spring stiffness is defined as a function of pressure and spring area. As the spring pressure and area change continuously during spring compression or expansion, the differential form is used for each of these.

Expanding on this work, Quaglia and Sorli [6] included an auxiliary volume. This necessitated the introduction of a continuity equation to account for mass flow between the air-spring and auxiliary volume. Different transmissibility magnitudes and resonant frequencies were obtained by changing the conductance or resistance between the air-spring and auxiliary volume. This method allowed tuning the suspension to yield an optimum point with low transmissibility characteristics.

Another area for which air-springs and auxiliary volumes are modelled is pneumatic vibrations isolators. In these devices, the air-spring assumes more of a cylinder and piston configuration. However, the equations defining the mass flow rate are for laminar flow and small variations between upstream and downstream pressures can be found in various Refs. [8–12].

In their paper, Toyofuku et al. [13] present equations of motion, continuity, state and energy for an air-spring and auxiliary chamber. Their differential form of the ideal gas equation is a practical means of obtaining the state equations. The energy balance equation also provides a basic guideline on the various forms of energy in the system.

The model equations presented in this article are based on some of the previous work as outlined above. Using a similar approach and including certain assumptions, the state equations of the model were derived from first principles. The aim was to accurately represent the air-spring and auxiliary volume to enable the design of prototype seat suspensions.

To develop a prototype air-spring with auxiliary volume for a suspension seat, tests specific to the application of the seat are required. Using the EM1 spectral class as defined in ISO 7096 (2000) [14] as the suspension seat vibration input, the suspension can be tested for its suitability for use in articulated or rigid frame dump trucks. To ensure the vibrations that are transmitted to test subjects or occupants are measured and evaluated correctly, ISO 2631-1 (1997) [15] is utilised. This international standard deals with the evaluation of human exposure to whole-body vibrations.

A method of communicating the dynamic performance of a seat is the seat effective amplitude transmissibility or 'SEAT' value. It factors in the vibration spectrum, seat transmissibility and human response to vibrations as outlined in Griffin [16]. For high vibration levels and at frequencies to which the human body is most sensitive, the attenuation needs to be the highest, and at frequencies where the human body is least sensitive, little or no attenuation is required. The SEAT value is defined as

$$\text{SEAT} = \frac{\text{Vibration on seat} \times \text{Frequency weighting}}{\text{Vibration on floor} \times \text{Frequency weighting}} \quad (1)$$

A SEAT value of greater than 100% indicates the seat amplifies the vibration and if the value is below 100%, the seat's dynamic behaviour has reduced the vibrations transmitted from the floor. This parameter is used to ascertain the suitability of the prototype for the specified application as will be determined in Section 5.

The following section presents the modelling of the air-spring and its state equations. Section 3 deals with the design objectives and Section 4 the design parameters and procedure. Section 5 presents the results and discussion and Section 6 the conclusion and recommendations for future work.

2. Modelling and derivation of state equations

The simulation model of the air-spring with an auxiliary volume was developed by deriving the state equations based on the thermodynamic, heat transfer and fluid mechanic principles encountered when dealing with gasses.

The model determines the spring force by means of the spring's internal pressure and incorporates the boundary work of the piston. The spring's pressure in turn is determined by a differential form of the ideal gas equation. The assumption of ideal gas behaviour is relevant since the relative pressure and temperature are in the regions where ideal gas behaviour can be assumed, namely $P_r \ll 1$ and $T_r > 2$ [17]. Thus, to obtain the change in pressure, one takes the ideal gas equation as an equation of state and differentiates it with respect to time.

To develop this model, the following assumptions were made:

- the air inside the spring is treated as an ideal gas;
- the area over which the spring pressure acts remains constant;
- heat transfer takes place between the spring and its surroundings;
- the unknown damping in the spring material can be represented by viscous damping;

- the flow in the restriction can be modelled by internal flow equations; and
- conservation of mass inside the air-spring and auxiliary volume.

In Quaglia and Sorli [6] both air-spring pressure and change in air-spring area were used to determine stiffness. For this study it was however assumed that due to the spring geometry, a rolling-lobe type air-spring, the change in spring pressure is more significant in influencing the spring stiffness than the change in area. Therefore, the air-spring area was taken as a constant in order to simplify the model.

To incorporate additional damping introduced over and above that provided by the flow restriction dynamics, a damping term is added to the state equation. This term was specifically included to account for any additional damping introduced to the experimental set-up through friction or flexing of the rubber diaphragm.

Since there is mass transfer between the air-spring and auxiliary volume, the continuity equation is incorporated into the model. The sign convention adopted for the air-spring is a positive mass flow out of the spring into the auxiliary volume as indicated in Fig. 1. The continuity equations can thus be defined as

$$\frac{dm_1}{dt} = -\dot{m} \text{ and } \frac{dm_2}{dt} = \dot{m} \quad (2)-(3)$$

The Reynolds number for flow passing through the restriction indicated that the flow was predominantly turbulent. Based on this, an equation was set up that defined the pressure loss occurring due to the flow restriction. It comprised of three components: friction, contraction and expansion losses. The minor losses were determined by the contraction and expansion coefficients for a square edged entrance and a sudden enlargement.

The major pressure loss was due to friction and was determined by the Darcy–Weisbach equation, valid for both laminar and turbulent flows [18]

$$P_{loss}(t) = f_{loss}\frac{l}{d}\frac{V(t)^2}{2g} \quad (4)$$

The friction factor, f_{loss}, was determined for $Re > 4000$ and completely turbulent flow with

$$f_{loss} = \left(-0.86\ln\frac{e}{3.7d}\right)^{-2} \quad (5)$$

Using the energy equation for pipe flow [18] and equating it with the head loss equation, neglecting the height difference of the capillary entrance and exits since this and the specific weight of air are very small, and then rearranging Eq. (4), one obtains an expression of the velocity. This equation is substituted into the mass flow rate equation and simplified. Considering the cross sectional area of the flow restriction as round, one obtains

$$\dot{m}(t) = \frac{(\pi/4)d^2\sqrt{2 \leftrightarrows \rho_{avg}(t)|P_1(t)-P_2(t)|}}{\sqrt{f_{loss}\frac{l}{d}+K_C+K_E}} + K_x \mathrm{sgn}(P_1(t)-P_2(t)) \quad (6)$$

where

$$\rho_{avg} = \frac{(P_1(t)+P_2(t))}{R(T_1(t)+T_2(t))} \quad (7)$$

Furthermore, the energy balance is set up for the spring volume. Noting that there is energy transfer between the spring and auxiliary volume, this needs to be accounted for in the energy balance. After substitution and simplification, one

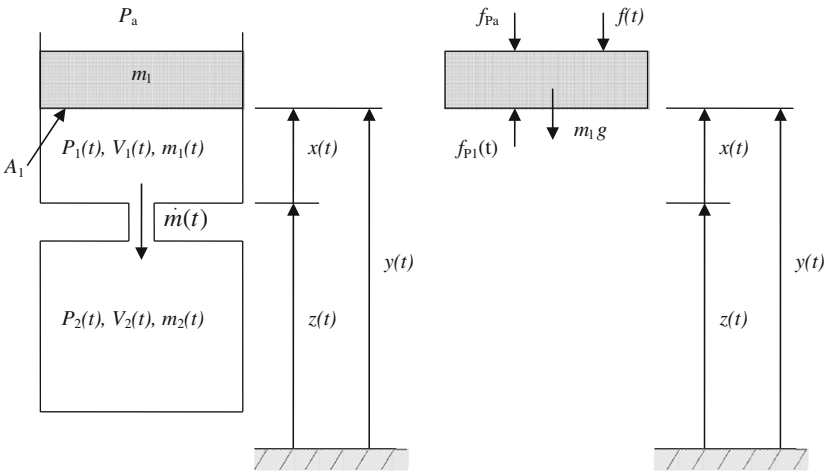

Fig. 1. Model of spring with auxiliary volume and free body diagram.

obtains a rate equation for the change in temperature:

$$\dot{T}_1(t) = -\frac{A_1 P_1(t)\dot{x}_1(t)}{m_1(t)C_v} - \frac{\dot{m}(t)C_p T_1(t)}{m_1(t)C_v} + \frac{QA_{s1}(t)(T_{s1} - T_1(t))}{m_1(t)C_v} \tag{8}$$

This temperature rate equation and the mass flow rate are substituted into the change in pressure equation and simplified making use of the ideal gas equation as follows:

$$\dot{P}_1(t) = -\left(1 + \frac{R}{C_v}\right)\dot{x}_1(t)\frac{P_1(t)}{x_1(t)} - \left(1 + \frac{C_p}{C_v}\right)\dot{m}(t)\frac{P_1(t)}{m_1(t)} + \frac{2}{r_1}\frac{R}{C_v}Q(T_a - T_1(t)) \tag{9}$$

Following a similar procedure for the auxiliary volume, but neglecting heat transfer, the pressure differential becomes

$$\dot{P}_2(t) = \left(1 + \frac{C_p}{C_v}\right)\dot{m}(t)\frac{P_2(t)}{m_2(t)} \tag{10}$$

The state equations derived for the spring and auxiliary volume model are summarised in Table 1.

To verify the numerical simulation model, experiments were performed on a suspension device consisting of an air-spring and auxiliary volume. For this device the air-spring supports a plate onto which weights can be loaded to test a variety of load cases (see Fig. 2). Furthermore, a seat can be mounted onto the apparatus so that human subjects can be used in testing. However, the tests performed were done using only the load plate and various weights, with no human subjects.

Table 1
State equations of complex spring model with auxiliary volume.

State equations	$\dot{y}(t) = \int \ddot{y}(t)\,dt$	(11)
	$\ddot{y}(t) = 1/m_1[A_1P_1(t) - A_1P_a - c(\dot{y}(t) - \dot{z}(t)) - f(t) - m_1 g]$	(12)
	$\dot{m}(t) = \frac{(\frac{\pi}{4})d^2\sqrt{2\rho_{avg}(t)\lvert P_1(t) - P_2(t)\rvert}}{\sqrt{f_{loss}\frac{l}{d}} + K_C + K_E} + K_x \mathrm{sgn}(P_1(t) - P_2(t))$	(6)
	$\rho_{avg}(t) = \frac{(P_1(t) + P_2(t))}{R(T_1(t) + T_2(t))}$	(7)
	$\dot{m}_1(t) = -\dot{m}(t)$, and $\dot{m}_2(t) = \dot{m}(t)$	(2,3)
	$\dot{P}_1(t) = -\left(1 + \frac{R}{C_v}\right)\dot{x}_1(t)\frac{P_1(t)}{x_1(t)} - \left(1 + \frac{C_p}{C_v}\right)\dot{m}(t)\frac{P_1(t)}{m_1(t)} + \frac{2}{r_1}\frac{R}{C_v}Q(T_a - T_1(t))$	(9)
	$\dot{P}_2(t) = \left(1 + \frac{C_p}{C_v}\right)\dot{m}(t)\frac{P_2(t)}{m_2(t)}$	(10)
States	$y(t), \dot{y}(t), m(t), P_1(t), P_2(t)$	

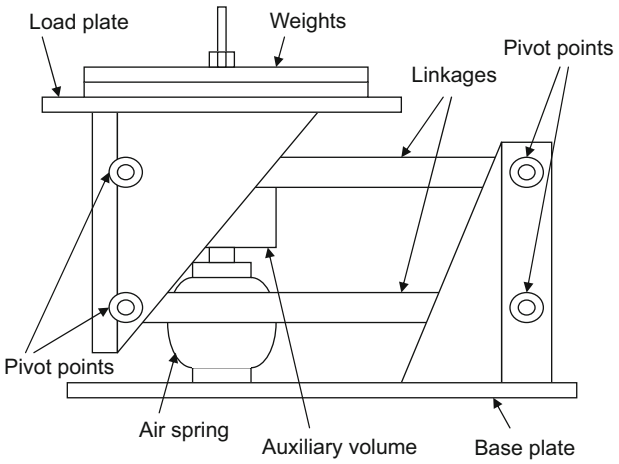

Fig. 2. Sketch of experimental apparatus.

To determine spring characteristics, the device was designed to approximate linear motion for the load and the air-spring. This was done using a Watt's linkage. The suspension apparatus was mounted onto a servo hydraulic actuated platform as illustrated in Fig. 3. In this way, the air-spring and auxiliary volume could be tested with desired vibration inputs.

The parameters of the model are listed in Table 2.

Comparing simulation model and experimental results in Fig. 4, the model predicted the trend as seen in the experimental apparatus; the simulation model and experimental results match up for the smallest diameter and as the diameter is increased, the model results follow the same trend. The most noticeable difference however, when overlaying the results for the simulation and experiment, is the minimum transmissibility and the lower natural frequency of the combined air-spring and auxiliary volume response. At the largest flow restriction diameter used here the simulation model showed an approximately 27% reduction in transmissibility and 21% lower system natural frequency than that obtained by tests.

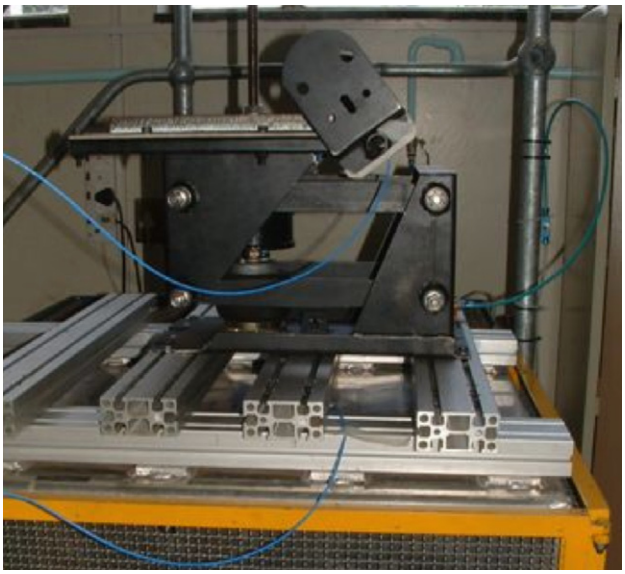

Fig. 3. Experimental apparatus on servo actuated hydraulic platform.

Table 2
Model parameters.

Air spring	A_1	7.85e−3	(m^2)
	x_{01}	0.075	(m)
	T_{01}	(273.15+15)	(K)
	m_1	36.2, 51.6, 67.1, 82.5	(kg)
	c	375, 420, 454, 528	(kg/s)
	P_{01}	146e3, 166e3, 185e3, 205e3	(Pa)
	g	9.81	(m/s^2)
	Q	30	($W/m^2\,K$)
Auxiliary volume	V_2	8.796e−4	(m^3)
	T_{02}	T_{01}	(K)
	P_{02}	P_{01}	(Pa)
Flow restriction	l	0.029	(m)
	d	1e−3; 1.5e−3; 2e−3; 2.5e−3; 3.5e−3; 5.5e−3	(m)
	e	0.005	(mm)
	K_C	0.5	(dimensionless)
	K_E	1	(dimensionless)
	K_x	0; 2	(dimensionless)
Air properties	R	287	(J/kg K)
	C_v	718	(J/kg K)
	C_p	1005	(J/kg K)
	T_a	(273.15+15)	(K)
	n	1.3	(dimensionless)

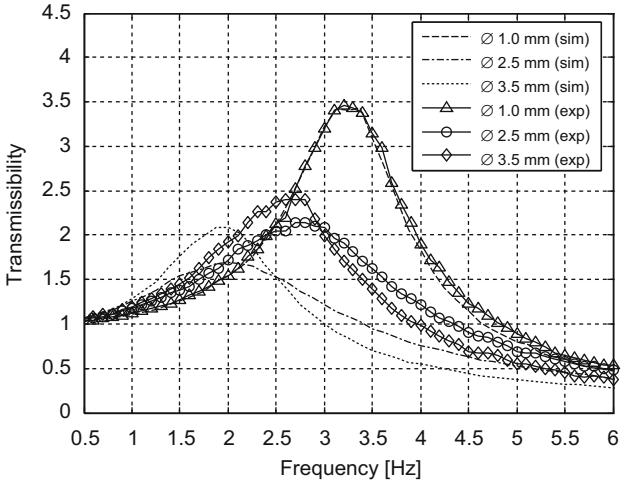

Fig. 4. Transfer function simulation and experiment load case 3 at an input level of 3 m/s^2 rms.

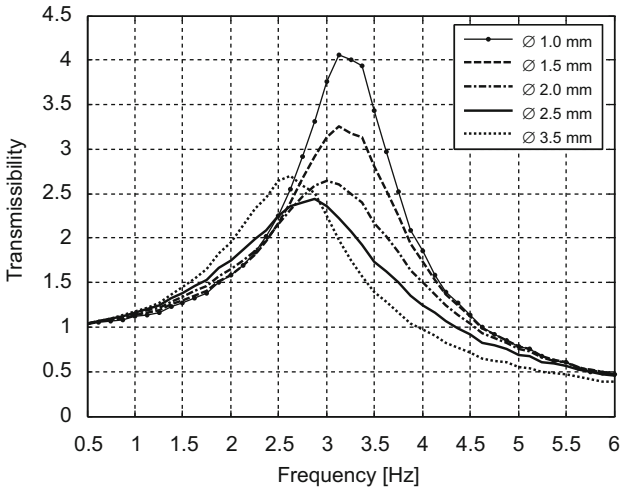

Fig. 5. Transmissibility curves of air-spring and auxiliary volume with $V/3$ and increased K_x.

Investigating this behaviour showed that the auxiliary volume had a pronounced influence on transmissibility magnitude and the lower natural frequency. Fig. 5 shows the system response for the original auxiliary volume size reduced by a third: $V/3$. Now the transmissibility curves of the experiment and simulation match, bar the higher transmissibility. This and the fact that an additional pressure loss coefficient, K_x, had to be introduced to obtain this result imply the flow restriction in the experimental device provides more damping than that initially modelled. In the light of this, it can be argued that the auxiliary volume model behaves as if the auxiliary volume is larger than it actually is. The simulation results thus predict a lower natural frequency and magnitude of transmissibility.

Despite the deviation in the lower natural frequency response of the model results for larger diameters, the model parameters were chosen as is for the design of the prototype air-spring for the suspension seat.

The advantage of using an auxiliary volume connected to a conventional air-spring for a seat suspension can be seen in Figs. 4 and 5, where for a diameter of 2.5 mm, in this case, the peak of the transmissibility curve is substantially less than for the case of the air-spring by itself and even smaller than that for larger diameter holes. As the low frequency resonance peak is a major contributor to the amplification of the vibration that occurs in this region this is an attractive feature when designing a seat suspension.

3. Design objectives

To develop the suspension for a specific application, an appropriate vibration input spectrum was used. The ISO 7096:2000(E) standard on *Earth-moving machinery—Laboratory evaluation of operator seat vibration* [14] provides various spectral classes of vibration inputs. The input used for this design application was the EM1 spectral class representing

vibration experienced in articulated or rigid frame dumpers. An input signal was used, the acceleration power spectral density of which had a similar rms acceleration content as that of the EM1 test. The acceleration power spectral density for the EM1 test is shown in Fig. 6.

An acceptable SEAT value is provided for each spectral class presented in ISO 7096 [14]. For EM1 spectral class, the standard stipulates a SEAT value of <1.1, meaning that no more than a 10% increase in the transmission of vibration through the seat is allowed. This value is calculated from the weighted acceleration power spectral density of the seat and floor as referred to in Section 1 by

$$SEAT = \left[\frac{\int G_{ss}(f)W_i^2(f)\,\mathrm{d}f}{\int G_{ff}(f)W_i^2(f)\,\mathrm{d}f}\right]^{1/2} \tag{13}$$

where $G_{ss}(f)$ and $G_{ff}(f)$ are the seat and floor acceleration power spectra and $W_i(f)$ is the frequency weighting for the human response to vibration, which is of interest [14].

As outlined in the introductory section, the weighting factor takes into account the fact that for high vibration levels and at frequencies to which the human body is most sensitive, the attenuation needs to be the highest and where the human body is least sensitive, little or no attenuation is required. A plot of the weighting function as stipulated by ISO 2631:1 [15] is presented in Fig. 7. This particular weighting is for vertical WBV.

According to Van der Westhuizen and Van Niekerk [19], the seat acceleration power spectral density $G_{ss}(f)$ can be determined by multiplying the floor acceleration power spectral density, $G_{ff}(f)$, by the magnitude squared of the transmissibility function obtained by tests obtained with the same magnitude acceleration rms values as obtained for

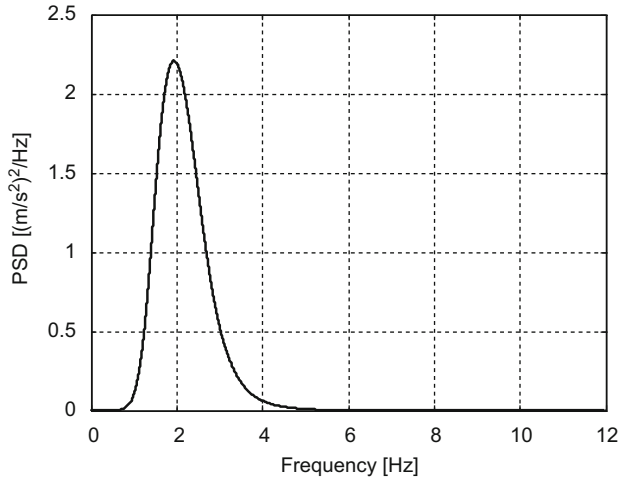

Fig. 6. Target PSD ($G^*p(f)$) for spectral class EM1—ISO 7096.

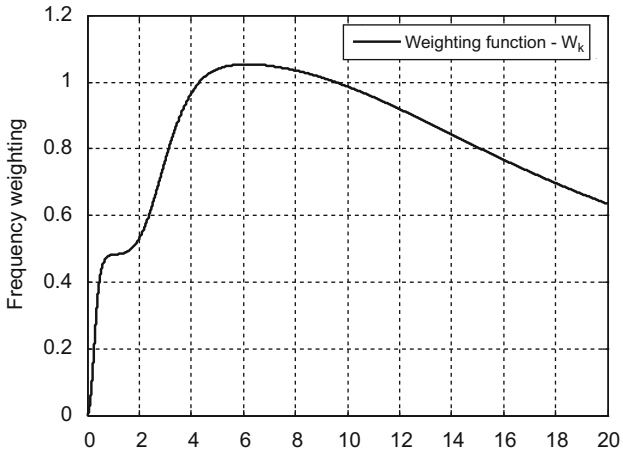

Fig. 7. Weighting function W_k for WBV in the z-direction—ISO 2631:1.

the EM1 test such that

$$G_{ss}(f) = G_{ff}(f)|H(f)|^2 \tag{14}$$

The SEAT value can thus be defined as

$$SEAT = \left[\frac{\int G_{ff}(f)|H(f)|^2 W_i^2(f)\,df}{\int G_{ff}(f) W_i^2(f)\,df}\right]^{1/2} \tag{15}$$

Considering the weighting function, it is clear that the transmissibility peak should be kept at as low a frequency value as possible, since at the lower frequency range, there is a lesser penalty incurred regarding transmitted vibration.

From the preceding discussion, it is recognised that the design objective is to lower the natural frequency of the system and decrease the transmissibility magnitude to the extent where the response of the system will result in a SEAT value of less than 1.1.

4. Design parameters and procedure

To design an air suspension that gives the desired response of good vibration isolation, specific design parameters or variables need to be identified. These enable the designer to systematically adjust the parameters to obtain the design objective of developing an air-spring and auxiliary volume suspension providing good vibration isolation.

Four main factors were identified when the models were developed that affect the air-spring and auxiliary volume combination frequency response. They are the

- air-spring effective area;
- suspended load;
- flow restriction diameter; and
- size of the auxiliary volume.

If a specific air-spring is used, the effective area becomes a constant, and as the load is considered a system input, the only remaining two parameters are the flow restriction diameter and auxiliary volume size, which can be considered as design variables.

The increase in the suspended load has the overall effect of decreasing the natural frequency of the system. Thus the range in operator weight needs to be taken into consideration, and to ascertain whether large variations occur with regard to the optimum diameter as the load was varied or if this is insignificant.

It was shown in the preceding sections that the increase in the flow restriction diameter from very small to larger ones decreased the system natural frequency and also the peak transmissibility. When changing this parameter, it is of interest to find the diameter size providing the lowest transmissibility. In light of this, the diameter size is considered a significant parameter, essential to obtain a low peak in the transmissibility.

The remaining factor to be considered is the auxiliary volume size. Literature indicates that the peak occurring at the largest diameter size is considered the peak of the combined volumes of the air-spring and auxiliary volume. It can thus be assumed that the larger the total volume, the lower the first natural frequency of the system. Fig. 8 illustrates the typical

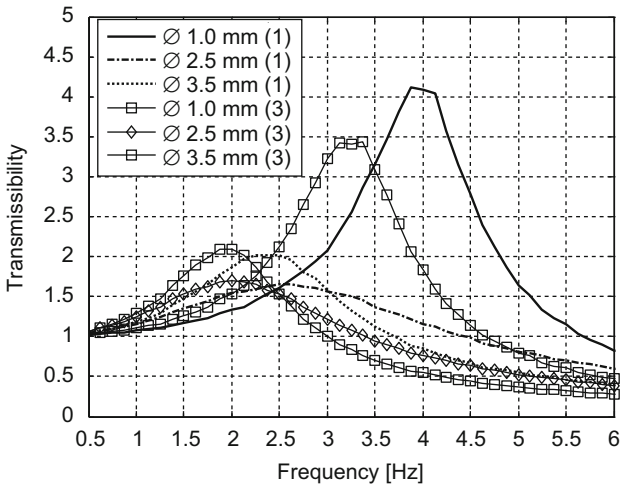

Fig. 8. Effect of changing flow restriction diameter and load on system response with load cases 1 and 3, load case indicated in parentheses ().

system response for two load cases as the flow restriction diameter is varied. Thus, to lower the natural frequency and peak transmissibility of the system, a larger auxiliary volume with a large diameter hole is required.

Having decided on the design variables and objective, a SEAT value below 1.1, the actual design procedure comprised a number of trial and error simulations to determine which combination of system parameters would provide the best results.

In the preceding paragraphs the auxiliary volume size and flow restriction diameter were recognised as the main design variables. The load was also varied to determine to which extent variation in operator weight would change the response. Two load cases, 1 and 3, were used again and two additional auxiliary volume sizes were selected besides the original volume, namely instances of twice and thrice the original volume size. The diameters ranged from 1.0 to 3.5 mm. This range allowed enough leeway to observe which diameter would be most suitable. Table 2 provides the model parameters used in this study.

Concerning the increase in the auxiliary volume size, attention needs to be turned back to the results in Section 2. It would seem evident that the simulation model behaves as if the auxiliary volume is larger than it actually is—the natural frequency and transmissibility magnitude are less than those in reality.

To try and match the simulation to the experimental results it was found that the volume should be decreased by a factor of about three. Since this would also require adjustment of the damping constants and flow loss coefficient, too much uncertainty would be introduced, making this approach less desirable. This merely substantiates the fact that more accurate modelling of the flow restriction would be necessary. It was therefore opted to rather continue with the present model for the design simulations.

Having established the design parameters and procedure, a number of simulations were performed to ascertain which combination of these parameters is best to obtain SEAT values below 1.1. The following section presents the results obtained from these simulations.

5. Results and discussion

Varying the selected design parameters, simulations proved that increasing the auxiliary volume showed a reduction in system lower natural frequency and reduction in peak transmissibility. The results when the volume is tripled are shown in Fig. 9. If the auxiliary volume size is increased, the lower natural frequency peak shifts to a new point with an even lower natural frequency. As predicted in the literature, this is due to the combined volumes of the air-spring and auxiliary volume. In addition to this, an interesting observation was a further reduction of the lowest peak of the transmissibility curves as the auxiliary volume was increased.

This response is ideal for the suspension seat to obtain a low SEAT value. Taking the transmissibility curve with the lowest peak obtained for the 2.5 mm diameter flow restriction, the SEAT value was calculated. The value obtained for this particular curve was 1.33 and thus too large to be acceptable.

Considering the 3.5 mm diameter flow restriction, a SEAT value of 1.05 was obtained. The fact that the transmissibility curve with a higher peak obtains a lower seat value is due to the combination of the floor acceleration power spectral density, the weighting function and the area under the transmissibility curve. Comparing the areas under the transmissibility curves for the 2.5 and 3.5 mm flow restrictions, it is evident that more vibration energy is transferred to the occupant for the 2.5 mm case, making this an unacceptable option. The transmissibility curve for the 3.5 mm

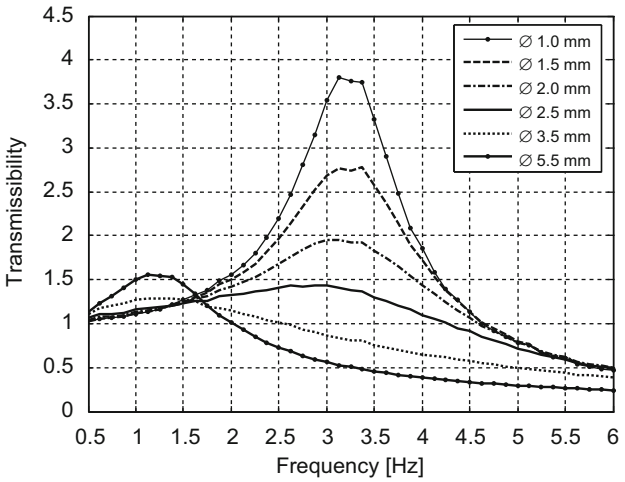

Fig. 9. System response with $3 \times V$ auxiliary volume size, load case 3 at 3 m/s^2 rms.

diameter falls away more rapidly in the critical region of 2 Hz and upward. The tripled volume and 3.5 mm flow restriction are therefore a suitable combination to adequately isolate an occupant from vibrations of spectral class EM1.

Referring back to Section 2, since the simulation models have lower transmissibility peaks compared to the experimental apparatus, the SEAT value is not necessarily representative of the real device. This section merely serves to illustrate the design procedure, not establish the actual SEAT value of the final suspension's characteristics. This will probably need to be determined using testing with human subjects.

When investigating the derivation of the system response for introducing varied loads, load case one in Fig. 10 shows the same trend exhibited by load case three when the volume was tripled. Here the diameter of 3.5 mm was marginally insufficient with a SEAT value of 1.11. The natural frequency occurring at this diameter was increased; however, peak transmissibility remained low. This indicated a reasonable independence regarding optimal hole-diameter and change in mass. Table 3 presents the SEAT values for four load cases.

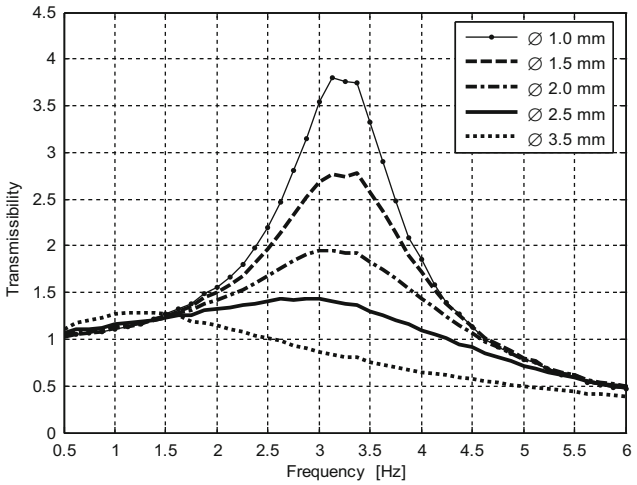

Fig. 10. System response with $3 \times V$ auxiliary volume size, load case 1 at 3 m/s^2 rms.

Table 3
SEAT values for various load cases and flow restriction diameters at $3 \times V$.

Load case (kg)	Ø2.5 mm	Ø3.5 mm	Ø5.5 mm
1. 36.2	1.248	1.114	1.091
2. 51.6	1.286	1.075	1.000
3. 67.1	1.326	1.051	0.929
4. 82.5	1.344	1.033	0.871

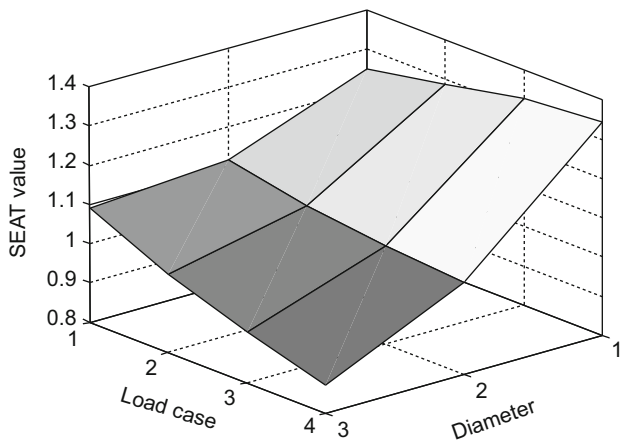

Fig. 11. Air-spring and auxiliary volume effectiveness in terms of SEAT value for $3 \times V$.

For illustrative purposes, the results in Table 3 are presented in Fig. 11 as a plot of SEAT values against load case and flow restriction diameter.

This plot clearly shows how, for a specific auxiliary volume size, the increase in mass reduces the SEAT value because of the reduction in the natural frequency of the system. This value can only be decreased to a certain level because the natural frequency has the lower bound of 0 Hz.

The increase of the flow restriction diameter also reduces the SEAT value. It will only do so up to a point since a further increase will cause a rise in the transmissibility peak. This peak will occur at the natural frequency for the combined volume of air-spring and auxiliary volume. It is probable that the area under the transmissibility curve will increase, again leading to a higher SEAT value. (This trend could not be illustrated since the model could not be reliably simulated at diameters of 6.5 mm or larger.)

These simulation results provide the design basis for an initial design of a prototype suspension system. Running tests on the prototype with given diameters would aid in validating the simulation model. For the prototype version, fine-tuning of the diameter size would then ensure the optimum diameter for the actual device. This could be done by varying the flow restriction diameter for different loads.

6. Conclusions and recommendations

Based on the work completed in this study the following conclusions can be drawn:

- It is possible to design an effective air-spring suspension for articulated and rigid-frame dump trucks by adding an auxiliary volume connected with an orifice to a standard air-spring.
- The air-spring and auxiliary volume simulation model presented here predicts the qualitative trend described in the literature; however, due to some limiting assumptions it does not exactly match the experimental response.

The auxiliary volume simulation model derived for this project has shown the distinct trend predicted in the literature of a reduction in peak transmissibility and natural frequency for increased flow restriction diameters [4]. However, deviation occurs for the simulation model at larger diameters from the experimental results. The transmissibility magnitude is decreased by 27% and the natural frequency lowered by 21%. Fig. 4 shows this discrepancy, which is assumed to arise from inaccurate modelling of the flow restriction.

By reducing the simulation model auxiliary volume by two-thirds and introducing a flow loss coefficient of K_x=2, the results match the experimental apparatus more accurately as seen in Fig. 5. The assumption of inaccurate flow modelling is thus supported as these changes imply that air passes through the restriction too easily. Despite these discrepancies, the auxiliary volume model proved to be a useful, initial optimisation tool.

The auxiliary volume model can be used as a basic design tool to obtain a SEAT value below 0.9 for a prototype seat suspension.

It may prove useful when conducting future research on this topic to further refine the simulation model and optimise the parameters used to model certain components of the system in order to match the system's behaviour more accurately. The model was developed using a number of simplifying assumptions. Whilst these are justifiable, one might be able to refine some of them to improve the accuracy of the simulation model.

One of the simplifications was the assumption of a constant spring area. Whilst this is a reasonable assumption due to the type of air-spring used, when working at the extremes of the spring's motion, where the peak transmissibilities are obtained, the spring's area is most likely different from the median position. Including the variation of the spring area as a function of displacement should introduce a closer correlation between the simulated results and those obtained by experiment. Thus, the discrepancies where the model was shown to deviate from the response of the experimental apparatus could be reduced further.

Another area that may prove worth focussing on is the flow restriction and related equations. As explained in previous paragraphs, the fact that the auxiliary volume appears larger than that in the experimental apparatus alludes to the fact that the air passage allows more free air movement between the two air volumes than is the case in reality. It may therefore be useful to investigate the modelling of the thermodynamic, heat transfer and particularly the fluid dynamic characteristics of the flow restriction.

Based on the research findings, the usefulness of the model as an initial tool to design an air suspension is encouraging, thereby motivating further research. Further research could include more accurate modelling of the spring area and investigating alternative flow restrictions models to determine their effect on transmissibility and particularly SEAT values. Integrating this design into a prototype seat for testing with human subjects and benchmarking against current air-suspension seats with dampers would be an obvious follow-on to the optimisation of the design.

In this project, a prototype seat suspension using an air-spring and auxiliary volume was designed for typical articulated or rigid frame dump trucks. Using the EM1 class vibration spectrum defined in ISO 7096 [12] for this type of vehicle, the suspension was optimised by varying the auxiliary volume size and flow restriction diameter. Referring to Table 3, a SEAT value of 0.871 was obtained for load case 4 with a $\varnothing$5.5 mm flow restriction. This process demonstrated

that the auxiliary volume model is both a practical design tool and that the combined air-spring and auxiliary volume system has the potential to be used as an effective seat suspension system.

References

[1] I. Hostens, K. Deprez, H. Ramon, An improved design of air suspension seats of mobile agricultural machines, *Journal of Sound and Vibration* 276 (1–2) (2004) 141–156.
[2] EU-Directive, Directive 2002/44/EC of the European Parliament and of the council of 25 June 2002, Official Journal of the European Communities.
[3] T. Ishitake, Y. Miyazaki, R. Noguchi, *Journal of Sound and Vibration* 253 (1) (2002) 31–36.
[4] M.H. Pope, D.G. Wilder, M. Magnussen, Possible mechanisms of low back pain due to whole-body vibration, *Journal of Sound and Vibration* 215 (4) (1998) 687–697.
[5] M.H. Pope, T.H. Hansson, Vibration of the spine and low back pain, *Clinical Orthopedics and Related Research* 279 (1992) 49–59.
[6] G. Quaglia, M. Sorli, Air suspension dimensionless analysis and design procedure, *Vehicle System Dynamics* 35 (2001) 817–829.
[7] A.A. Kornhauser, Dynamic modeling of gas springs, *Transactions of the ASME, Journal of Dynamic Systems, Measurement and Control* 116 (1994) 414–418.
[8] G. Quaglia, M. Sorli, Experimental and theoretical analysis of an air spring with auxiliary reservoir, *Proceedings of the 6th International Symposium on Fluid Control Measurement and Visualisation* (*FLUCOME 2000*), Sherbrooke, Canada, August 2000.
[9] B.I. Bachrach, E. Rivin, Analysis of a damped pneumatic spring, *Journal of Sound and Vibration* 86 (2) (1983) 191–197.
[10] E.I. Rivin, *Passive Vibration Isolation*, Professional Engineering Publishing Limited, United Kingdom, 1983.
[11] C. Erin, B. Wilson, J. Zapfe, An improved model of a pneumatic vibration isolator: theory and experiment, *Journal of Sound and Vibration* 218 (1) (1998) 81–101.
[12] J.-H. Lee, K.-J. Kim, Modeling of nonlinear complex stiffness of dual-chamber pneumatic spring for precision vibration isolations, *Journal of Sound and Vibration* 301 (2007) 909–926.
[13] K. Toyofuko, C. Yamada, T. Kagawa, T. Fujita, Study on dynamic characteristic analysis of air spring with auxiliary chamber, *JSAE Review* 20 (1999) 349–355.
[14] International Organization for Standardization, Earth-moving machinery—laboratory evaluation of operator seat vibration, ISO 7096, 2000.
[15] International Organization for Standardization, Mechanical vibration and shock – evaluation of human exposure to whole-body vibration – part 1: general requirements, ISO 2631-1, 1997.
[16] M.J. Griffin, *Handbook of Human Vibration*, Academic Press Ltd., California, 1990.
[17] Y.A. Çengel, M.A. Boles, *Thermodynamics – An Engineering Approach*, fourth ed, McGraw-Hill, New York, 2002.
[18] M.C. Potter, D.C. Wiggert, *Mechanics of Fluids*, third ed, Brooks/Cole, California, 2002.
[19] A. Van der Westhuizen, J.L. Van Niekerk, Verification of seat effective amplitude transmissibility (SEAT) value as a reliable metric to predict dynamic seat comfort, *Journal of Sound and Vibration* 295 (2006) 1060–1075.